

## **SUPERSONIC COMBUSTION EXPERIMENTS FOR CFD MODEL DEVELOPMENT AND VALIDATION (INVITED)**

A. D. Cutler\*, P. M. Danehy†, S. O'Byrne‡, C. G. Rodriguez§, J. P. Drummond\*\*

*NASA Langley Research Center, Hampton, VA 23681*

### **ABSTRACT**

This paper briefly reviews a number of experiments suitable for the screening, development and validation of turbulence models used in computational fluid dynamics (CFD). Then, two sets of experiments conducted for this purpose by the authors are presented. The first is a compressible axisymmetric jet in which a central jet of helium mixes with a surrounding coflow of air. The second is a supersonic combustor. Various instrumentation techniques have been employed with the axisymmetric jet, whereas the dual pump coherent anti-Stokes Raman spectroscopy technique has been applied to the combustor. Experiences in trying to calculate these flows, and set model constants, are reviewed.

### **INTRODUCTION**

Historically, a combination of one-dimensional computations, semi-empirical modeling, and the results of technology demonstration experiments have been used to design hypersonic airbreathing engines, such as ramjets, scramjets, and combined-cycle engines. More recently, fully three-dimensional computational fluid dynamics (CFD) codes are instead being used<sup>1</sup>. These flows are turbulent, reacting, and may have large regions of flow reversal. They exhibit shock waves, shock-boundary layer interactions, and other compressibility effects. Owing to these complexities, many simplifying assumptions are typically made to make the computer codes fast enough for practical engine design.

For computational efficiency, the Reynolds averaged (time-averaged) form of the Navier-Stokes (RANS)

equations is typically used. These equations introduce new variables that must be modeled, such as the Reynolds stress tensor, and the turbulent heat and mass flux vectors. Reduced (simplified) chemical kinetics models are required to further reduce computational requirements, especially for hydrocarbon fuel combustion, and models for the interactions between the turbulence and the chemistry may be required. These models, in turn, employ other statistical quantities of the turbulence in their development, and have to be empirically calibrated or at least empirically validated. Other CFD techniques, such as large eddy simulation, also employ empirically calibrated or empirically validated statistical models, albeit such techniques may be less sensitive to errors in their empirical model coefficients.

Experimental data are required in the development, validation, and screening of these models, and for the validation of the CFD codes that employ them. These models typically employ multiple coefficients that must be established empirically. For development of models, measurements of the quantities being modeled (Reynolds stress tensor, turbulent heat and mass flux vectors, etc.) and also the independent variables of the models (parameters of the mean flow field) would be ideal. More often, the situation is that modeling coefficients are inferred from measurements of mean flow quantities and with only limited turbulence measurements. Unfortunately, this limited data does not always allow model assumptions to be thoroughly tested.

Interaction with CFD modelers has identified the following requirements for a data set suitable for model

\* Associate Professor, The George Washington University, M.S. 905. Senior Member AIAA

† Research Scientist, Advanced Sensing and Optical Measurement Branch, Mail Stop 236. Member AIAA

‡ Postdoctoral Fellow, UNSW@ADFA, Canberra, ACT, 2600, Australia, formerly NRC Postdoctoral Fellow at NASA Langley Research Center. Member AIAA

§ Senior Engineer, ATK GASL, MS 353X. Member AIAA.

\*\* Senior Research Scientist, Hypersonic Airbreathing Propulsion Branch, MS 197. Associate Fellow, AIAA.

Copyright © 2004 by the American Institute of Aeronautics and Astronautics Inc. The U.S. Government has a royalty-free license to exercise all rights under the copyright claimed herein for Governmental purposes. All other rights are reserved by the copyright owner.

development and validation:

- (i) The flow field contains some of the features relevant to high-speed engine flow paths, such as supersonic mixing and combustion, and supersonic combustion with embedded regions of subsonic or recirculating flow.
- (ii) The flow fields have well-controlled and well-described model geometries, and inflow and wall boundary conditions.
- (iii) The flow field is relatively simple, to keep both the quantities of data acquired and its' interpretation manageable. A simple flow field allows data to be concentrated in a few spatial locations, increasing measurement precision in turbulence statistics.
- (iv) The data contains measurements of multiple flow-field mean flow and turbulence quantities, especially those quantities modeled in the RANS equations.
- (iv) Experimental uncertainties are well quantified, preferably verified by redundant measurements (by different techniques).
- (v) The data should be of an adequate precision. Acceptable precision levels depend on the existing uncertainty in the in the models, which may be high if no other data is available. It also depends on the sensitivity of the measured quantities to the model coefficients: typically mean flow quantities will be less sensitive to the coefficients than will the quantities actually being modeled (Reynolds stress tensor, turbulent heat and mass flux vectors, etc.). This is fortunate since measurement precision is typically poorer for turbulence quantities.

We consider now the past research in the development of such data bases. There has been a great deal of research conducted in the area of low speed turbulent flow, subsonic diffusion flames, etc., that will not be considered here, although this must necessarily have input to the modeling. The following works represent some of the highlights of the relevant existing literature for high-speed flows with mixing or mixing and combustion. This list is not meant to be an exhaustive or critical review but, rather, illustrative.

The early fundamental work on supersonic planar mixing layers was by Papamoschou and Roshko<sup>2</sup>, Dimotakis<sup>3</sup>, and others. More recent work includes Mungal<sup>4,5,6</sup> and his collaborators at Stanford University. This work showed definitively that compressibility has a large effect on mixing, and provided physical inputs to the models. There is a considerable body of work in the area of supersonic jets, much of which has been conducted in an attempt to understand and model aeroacoustic noise. This includes the work of Seasholtz and his collaborators at NASA Glenn Research Center<sup>7,8,9</sup>, which contains credible measurements, not only of mean flow quantities, but of turbulence statistical quantities (density and velocity fluctuations). Several experiments in the area of

scramjet-type flows have been conducted at the University of Virginia, including studies of mixing without combustion and of supersonic combustion<sup>10</sup>. Spatially resolved measurements were reported of mean pressure, temperature, three components of velocity, and injectant mole fraction in a non-combusting scramjet-type flow using planar laser induced iodine fluorescence<sup>11</sup>. Although this was a non-combusting case, this data set has been widely used in the development and validation of models for scramjets. In a combustor experiment, Goynet et al. report measurements using particle-imaging velocimetry of mean streamwise velocity in a dual-mode ramjet<sup>12</sup>, but this data was limited. Neither of these two experiments provided turbulence statistics. Detailed studies of rocket chamber and rocket-based combined-cycle engine flow fields were conducted by Santoro, and his collaborators at Penn State University<sup>13,14</sup>. Techniques used include Raman spectroscopy for species concentration and laser-Doppler velocimetry for velocity. In this application, the Raman technique provided measurements of mean flow temperature and species concentration, however, the measurement precision was not high. International work in this area includes measurements in scramjet combustors conducted at ONERA (France) and DLR (Germany) using coherent anti-Stokes Raman spectroscopy (CARS)<sup>15</sup>, and other non-intrusive techniques.

The authors of the present proposal have recently developed data in support of NATO Research and Technology Organization Working Group 10, Subgroup 2 activities. This working group subgroup was formed in June 1998 to address selected technology issues related to supersonic combustion ramjets (scramjets). Two experiments were performed at NASA Langley Research Center for CFD validation and model development. The first experiment studied a supersonic coaxial jet with central helium jet and air coflow: the helium-air mixing layer was compressible. Conventional probe based techniques (gas sampling, Pitot probes, total temperature probes) and a non-intrusive velocimetry technique (RELIEF) were employed and the results are presented in Refs.16,17. CFD calculations are reported in Refs.18,19. The second experiment<sup>20</sup> was a study of a supersonic combustor with single H<sub>2</sub> fuel injector conducted in Langley's direct connect supersonic combustion test facility (DCSCTF<sup>21</sup>). The CARS technique was used to measure mean and fluctuating temperature in several planes of two flows, one piloted and one unpiloted. Modern design of experiment (MDOE) techniques, including response surface methodology (RSM), were applied in this experiment.<sup>22, 23</sup> In a follow-on experiment, the dual-pump CARS technique was used to measure, in addition to temperature, concentrations of N<sub>2</sub>, O<sub>2</sub>, and H<sub>2</sub> in this combustor<sup>24,25,26</sup>. CFD computations of

the flowfield and comparisons to the experiment have also been presented<sup>19,27</sup>.

The state of the art may be summarized as follows. Many experiments have been conducted that have little or no value for model validation because inflow properties and geometry are not well-controlled or well known. Others have only a limited range of measurements, and typically no turbulence statistical information, or lack the required detail and precision in the measurements. These deficiencies are not surprising, due to difficulties in making the required measurements. Measurement techniques that have been the mainstay in low speed flows, such as hot-wire anemometry or particle-based velocimetry techniques, are not useful or are problematic in high-speed, combustor flow. Additional factors that affect the quality and availability of data are that test facilities tend to have poorer optical/probe access and are very expensive to build and operate.

The purpose of this paper is to critically review the recent work of the authors, especially in relation to the outlined requirements for data bases. Since several RANS CFD calculations will be presented in this paper, we will discuss the method employed. We will discuss our supersonic (non-combusting) coaxial jet experiment, and recent efforts to model this flow. Finally, we will discuss our measurements in the SCHOLAR supersonic combustor model. In this context, we will describe the experimental techniques employed, especially the dual Stokes Coherent anti-Stokes Raman spectroscopy (CARS) technique and the use of RSM.

### **CFD MODELING**

Computations have used VULCAN,<sup>28</sup> a structured, finite-volume CFD code that solves the Favre-averaged Navier-Stokes equations. The flows are turbulent and variants of Wilcox's<sup>29</sup> 1998 high Reynolds number mode  $\tilde{k} - \tilde{\omega}$  turbulence model are used. The compressibility correction proposed by Wilcox, and Wilcox's generalization of Pope's modification to the  $\tilde{k} - \tilde{\epsilon}$  model, which attempts to resolve the "round jet/plane jet anomaly", are used in some cases. Details of the numerical procedures, computational grids, and so forth will not be discussed: the reader is referred to the original publications. The focus of the CFD element of this paper is turbulence and combustion modeling.

It is of interest in the current context to summarize the method by which the model coefficients were set by Wilcox, as outlined Section 4.4 of Ref. 29. The model has five coefficients:  $\alpha$ ,  $\beta$ ,  $\beta^*$ ,  $\sigma$ , and  $\sigma^*$ . Experimental observations of decaying homogeneous, isotropic turbulence fixed the ratio of  $\beta^*$  to  $\beta$ . The requirement to be consistent with the law of the wall, taken together with

experimental measurements of the ratio of the turbulent shear stress to the turbulent kinetic energy in the wall region, yielded values for  $\alpha$ ,  $\beta$ , and  $\beta^*$ . There are no such simple methods for setting the values of  $\sigma$ , and  $\sigma^*$ , which regulate the turbulent diffusion of  $\tilde{\omega}$  and  $\tilde{k}$  respectively.

The value of  $\sigma$  was chosen to provide good solutions in the viscous layer of a boundary layer, independent of  $\sigma^*$ . The value of  $\sigma^*$  was chosen to match CFD calculations to measurements of the wake strength parameter in turbulent boundary layers in adverse pressure gradients. Wilcox's round-jet/plane-jet anomaly correction is a factor on  $\beta$  that is unity in two-dimensional flows. The compressibility correction modifies  $\beta$  and  $\beta^*$ , and is calibrated by matching calculations to the experimentally determined reduction in planar shear layer growth rate with increasing convective Mach number.

The turbulent heat and mass flux vectors are computed from the local temperature and species mass fraction gradients, and the eddy viscosity, by taking the turbulent Prandtl ( $Pr_T$ ) number and turbulent Schmidt ( $Sc_T$ ) number to be constants. According to Wilcox, common values of  $Pr_T$  are 0.9 in boundary layers (near the wall), and  $\sim 0.5$  in free shear layers and at the edge of boundary layers. This is consistent with the results reported by Bagheri and White<sup>30</sup> for incompressible boundary layers. Calhoon et al.<sup>31</sup> have inferred  $Pr_T$  distributions from large-eddy simulations of planar shear layers, and report values of  $Pr_T$  that are low and vary across the layer at low convective Mach number, but are more uniform and approach 0.9 at high Mach number. There appears to be little data for  $Sc_T$  in the literature.

### **SUPERSONIC COAXIAL JET**

The supersonic (non-combusting) coaxial jet experiment was conducted in NASA Langley's Mixing Studies Facility. The flow consists of a center jet of a light gas (a mixture of 5% O<sub>2</sub> and 95% helium by volume) and coflow jet of air. It is formed by an axisymmetric nozzle consisting of outer and center bodies. The passage between these bodies forms the coflow nozzle and the center body contains the center jet nozzle. Contours are designed by the method of characteristics to produce 1-D flow at the nozzle exit. The jet discharges into the ambient air with uniform exit static pressure of 1 atmosphere. The presence of O<sub>2</sub> in the center jet is to allow the use of a flow-tagging technique (RELIEF, Raman excitation plus laser-induced electronic fluorescence<sup>32</sup>) to measure velocity non-intrusively.

Both center jet and coflow are nominally Mach 1.8, but, because of the greater speed of sound of the center jet, its velocity is more than twice that of the coflow. The two-stream mixing layer which forms between the center

jet and the coflow near the nozzle exit is expected to be compressible, with a calculated convective Mach number<sup>2</sup> (the average value for the center jet relative to the mixing layer and for the mixing layer relative to the coflow),  $M_c$ , of 0.7. This convective Mach number is in a transitional range where shear layer growth rates fall rapidly from incompressible rates with increasing  $M_c$ .

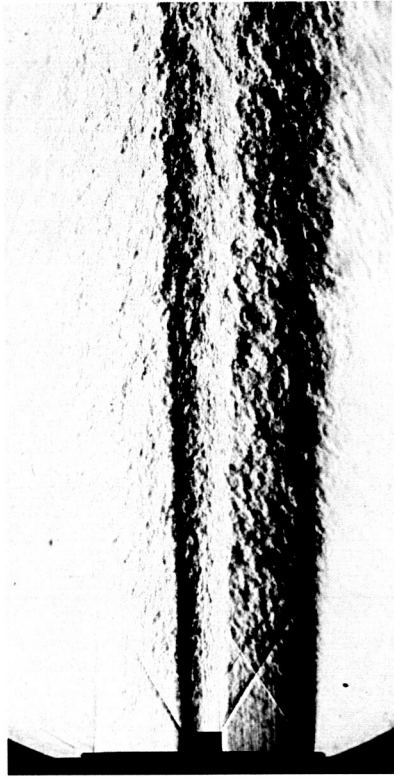


**Figure 1 Supersonic coaxial jet (Schlieren, Ref. 16).**

The jet flow is shown in Fig. 1, which is a schlieren image. Vertical dark and bright bands may be seen at the left and right edges respectively of the center jet, and also at the right and left edges of the coflow jet, due to large transverse gradients of refractive index. Notice also the shock/expansion wave structure emanating outward from the center-body lip. In addition to the flow visualization, the flow field has been surveyed using various techniques. Conventional probe techniques include miniature Pitot ( $\pm 0.5\%$  uncertainty), gas sampling for mole fraction center jet gas ( $\pm 1.5\%$  uncertainty), and total temperature ( $< 1\%$  uncertainty). In addition, the RELIEF<sup>32</sup> O<sub>2</sub> flow tagging technique has been used to provide multiple measurements of (instantaneous) axial component velocity, which have been used to obtain mean and root-mean-square fluctuating velocity ( $\bar{u}$ ,  $\sqrt{u'^2}$ ) (uncertainty  $\sim \pm 3\%$ ).

A series of CFD calculations of the nozzle and jet flow using the VULCAN code have been presented in Ref. 18. The sensitivity of the results to the use of several different turbulence models, including the  $\tilde{k} - \tilde{\omega}$  model, the sensitivity to variation in  $Pr_T$  and  $Sc_T$  (these were assumed to be equal) and to the use (or omission of) the Pope and the compressibility corrections within the  $\tilde{k} - \tilde{\omega}$  model. The best results were obtained with the  $\tilde{k} - \tilde{\omega}$  model using the Pope correction but not the compressibility correction, and with  $Pr_T = Sc_T = 0.75$ . However, the results were unsatisfactory. All cases underpredicted mixing at the outer edge of the center jet and at the interface of the coflow with the coflow/ambient mixing layer, with severe discontinuities in slope of mole fraction center-jet gas and Pitot pressure being observed.

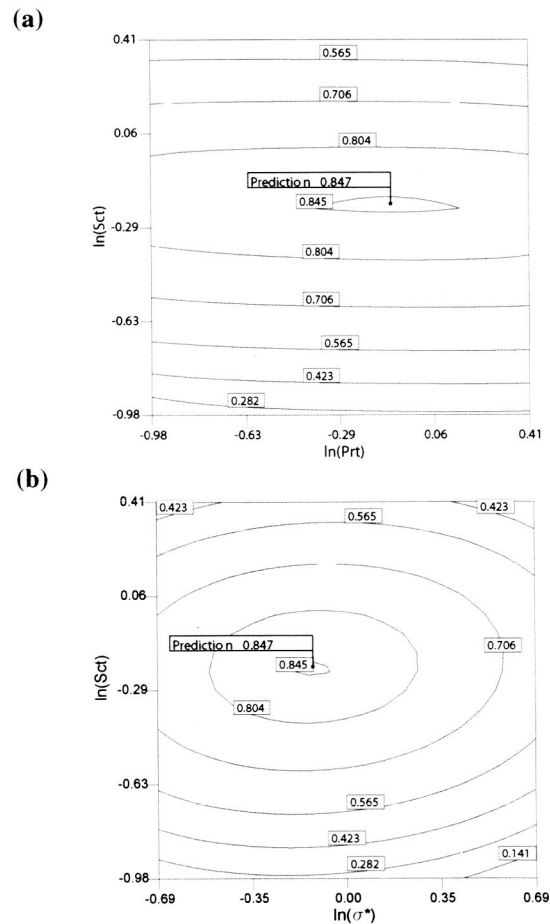


**Figure 2 Contours of desirability (no compressibility correction cases) showing optimum 1: (a) constant  $\sigma^*=0.9$ , (b) constant  $Pr_T=0.90$ .**

The above-described calculations were published prior to the RELIEF measurements becoming available.



Subsequent comparison between the published best calculation and experiment revealed an interesting result. It was found that the width of the centerjet/coflow mixing layer thickness was substantially less in the CFD-computed  $\sqrt{\frac{2}{3}\tilde{k}}$  than in the measured  $\sqrt{u'^2}$  at several streamwise locations. (Note that  $\sqrt{\frac{2}{3}\tilde{k}}$  is a similar quantity to  $\sqrt{u'^2}$ , and is equal to it for isotropic incompressible turbulence.) This suggested that the effect of the parameter  $\sigma^*$ , which regulates the turbulent diffusion of  $\tilde{k}$  in the  $\tilde{k}$  equation, be also investigated. Consequently, an optimization was performed, including this parameter.

	Optimum 1		Optimum 2		Worst
$Pr_T$	0.9		0.6		0.75
$Sc_T$	0.82		0.80		0.375
$\sigma^*$	0.9		1.3		1.0
Comp corr	No		Yes		Yes
Pred/actual	P	A	P	A	A
$R_{x,121}\times 10^4$	5.6	3.9	3.0	1.5	69.
$R_{x,261}\times 10^4$	5.9	1.3	3.1	2.4	120.
$R_{Pr,121}\times 10^4$	2.0	1.1	3.5	3.4	37.
$R_{Pr,261}\times 10^4$	2.2	0.82	4.3	3.8	39.
$R_{T,101}\times 10^4$	0.46	0.38	0.75	0.9	16.

**Table 1 Locations of optima and response function values.**

A matrix of computational cases was generated using commercial software written for design of experiments<sup>33</sup>. Each of these cases was calculated using the same methods as described in Ref. 18, and the  $\tilde{k} - \tilde{\omega}$  model with Pope's correction was employed. A series of 11 cases employed the compressibility correction while a second series of 16 cases did not. The parameters  $Pr_T$ ,  $Sc_T$ , and  $\sigma^*$  were varied in the ranges 0.375 to 1.5, 0.375 to 1.5, and 0.5 to 2.0 respectively. The results of the CFD calculations were interpolated to the measurement point locations. A "response" function,  $R_x$  for mole fraction surveys and  $R_{Pr}$  for Pitot probe surveys, was formed for each experimental survey considered by taking the mean square deviation between experimental points and the interpolated CFD calculation. Results were obtained for Pitot and gas sampling surveys at  $x=121$  mm and  $x=261$  mm, and for a total temperature probe survey at  $x=101$  mm (only one survey was performed with that probe). Within the design of experiment software, the logarithm of the response functions were fit to quadratic function

response surfaces (5 surfaces, 2 each for the two Pitot and gas sampling surveys, one for the total temperature survey). Independent variables for these fits were  $\ln(Sc_T)$ ,  $\ln(Pr_T)$ , and  $\ln(\sigma^*)$ . Thus, the quadratic function has 9 coefficients to be fit. The standard error of the fits for the case with compressibility correction ranged for the various response functions from 8% to 29%. Without compressibility it was 32% to 52%, higher due to the greater number of points being fit relative to the number of coefficients (if only 9 points were fit, the surface would inevitably pass through all the points with no error). However, this higher standard deviation is not really reflective of the uncertainty, which is likely to be higher for the surface fit for the case with fewer points. This standard error is quite high, but it is expected to be acceptable for the purposes of optimization.

An optimization was then performed, utilizing these surfaces, to jointly minimize the set of response functions. The "desirability" function being maximized is the renormalized (reciprocal) geometric mean of the 5 response functions. Once the "optimum" was found the CFD calculation was rerun for the optimum  $Sc_T$ ,  $Pr_T$ , and  $\sigma^*$ , and the response functions were recomputed and compared to the prediction. Figure 2 shows contour plots of the desirability function and Table 1 summarizes the variables and response functions at the optima. A single optimum was found for each case (with and without compressibility correction). Also shown in the table is the worst of the matrix of cases computed, to give an idea of how high the response functions go within the parametric space. It may be seen in Fig. 2 that the desirability is rather insensitive to  $Pr_T$ ; this is not surprising given a small difference in total temperature between the air coflow and the helium centerjet, and the resultant low turbulent heat fluxes (a large percentage error in heat flux will not severely affect the Pitot or mole fraction in the flow). The desirability is most sensitive to  $Sc_T$ , and a little less sensitive to  $\sigma^*$ . Optimum  $Sc_T$  is about 0.80-0.82, while the optimum  $\sigma^*$  depends on whether the compressibility correction is chosen, but is in both cases significantly greater than Wilcox's recommended value of 0.5.

Figure 3 compares experimental data and CFD calculations using the two optimized sets of  $Pr_T$ ,  $Sc_T$ , and  $\sigma^*$ . Mole fraction center jet gas is shown in (a), Pitot pressure (normalized with coflow plenum pressure) is shown in (b), total temperature normalized with coflow plenum temperature is shown in (c). Agreement between CFD and experiment is generally good, perhaps a little better for Optimum 1. However, fewer CFD runs were used in the surface fits for the compressibility case (presumably the surface fit was less accurate), so perhaps

a better optimum could have been found for that case. Figure 3(d) compares the RELIEF measurements of  $\sqrt{u'^2}$  to calculations of  $\sqrt{\frac{2}{3}\tilde{k}}$ . Some discrepancies between CFD and measurement are possibly attributable to lack of isotropy.

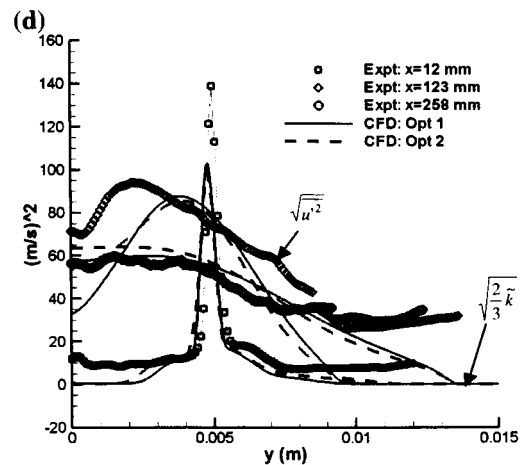
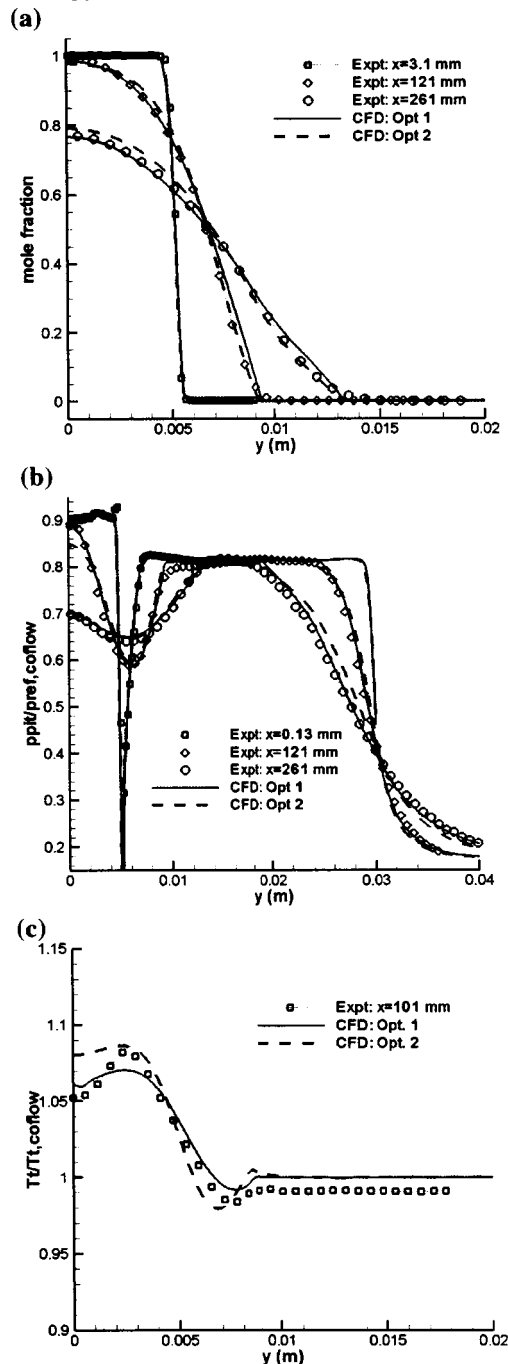


**Figure 3 Comparisons between CFD with optimized constants and experiment for axisymmetric jet: (a) mole fraction centerjet gas, (b) Pitot pressure, (c) total temperature, (d) fluctuating velocity**

(experimental  $\sqrt{u'^2}$ , Ref. 17, and CFD  $\sqrt{\frac{2}{3}\tilde{k}}$ ).

Note the higher baseline (freestream) levels of turbulence in the experiment. Freestream turbulence levels are believed to be low at the nozzle exit, and the baseline measurement level at  $x=0.13$  mm of 5-10 (m/s) is believed attributable to instrument precision (indeed, this is very low). However, further downstream, freestream levels rise considerably for reasons unknown, and this is not reproduced in the calculation.

It is not possible, based on this analysis, to determine which of the two combinations of parameters/models, if either, is more likely to be more generally applicable. It is not suggested that the higher value of  $\sigma^*$  should replace Wilcox's recommended value of 0.5 in other applications. Indeed, there appears to be a small but unfavorable effect of these higher values on the calculation in the coflow nozzle, at the outer edge of the centerbody boundary layer. A slightly increased rate of spreading is observed there that appears inconsistent with the Pitot data at the  $x=0.13$  mm.

#### **SUPERSONIC COMBUSTOR EXPERIMENT TEST FACILITY AND MODEL**

This experiment was conducted in Langley's DCSCF<sup>21</sup>. "Vitiated air" is produced at high pressure in the "heater": O<sub>2</sub> and air are premixed and H<sub>2</sub> is burned in the mixture. Flow rates are selected so that the mass fraction of O<sub>2</sub> in the resulting products is the same as that of standard air, and the enthalpy is nominally that of Mach 7 flight. The vitiated air is accelerated through a water-cooled convergent-divergent nozzle and enters the test

model.

A study of the flow at the exit of the facility nozzle was conducted<sup>34</sup>. A probe rake was employed to map the exit Pitot pressure. Additionally the flowfield at the exit of the nozzle was visualized. Silane ( $\text{SiH}_4$ ) was added to the heater hydrogen and burned to form silica particles in the heater. The particles were illuminated by a pulsed laser-light sheet and imaged with a CCD camera. The flow appeared well mixed.

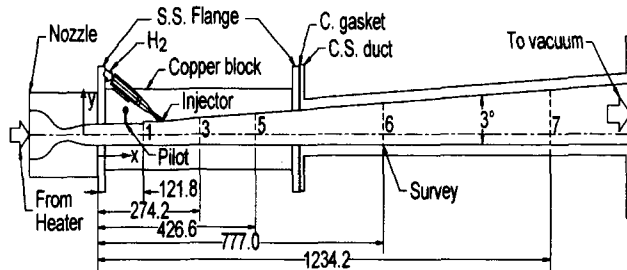


**Figure 4 Supersonic combustion experiment model**

The test model is shown in Fig. 4. There are two main sections: the copper section upstream and the carbon steel section downstream. Stainless steel flanges and carbon gaskets separate these sections from each other and the nozzle. The internal passage, from left to right, has a constant area segment 38.6 mm high, a 4.8 mm outward step at the top wall, a 44 mm constant area segment followed by a constant  $3^\circ$  divergence of the top wall. The span is constant at 87.88 mm. Small pilot fuel injector holes were not employed in this experiment. The main fuel injector is located just downstream of the start of the  $3^\circ$  divergence and the injection angle is  $30^\circ$  to the opposite wall. The injector nozzle is designed by the method of characteristics to produce Mach 2.5, 1D flow at the injector exit. Hydrogen injection is provided at a temperature of  $302 \pm 4$  K, and equivalence ratio of  $0.99 \pm 0.04$ .

The duct is uncooled; however, the wall thickness of the copper duct is greater than 32 mm and the carbon steel duct wall thickness is 19 mm. Thus, run times fueled in excess of 20 s are possible (and much greater if unfueled). With atmospheric temperature air flowing in the model between runs, runs could be repeated every 10 - 15 minutes.

The model is equipped with slots to allow optical access to the duct. The slots are in pairs, one on each side of the duct, 4.8 mm wide, extending the full height of the duct. When not in use the slots are plugged flush to the wall. Windows covering the slots are mounted at the end of short rectangular tubes. The model is additionally instrumented with both pressure taps and wall temperature probes.

## CARS DIAGNOSTICS

The dual-pump CARS method developed by Lucht<sup>35,36</sup> was used to simultaneously measure temperature and the absolute mole fractions of  $\text{N}_2$ ,  $\text{O}_2$ . Lucht's method has also been extended measure  $\text{H}_2$ . Conventional broadband  $\text{N}_2$  CARS uses two spectrally-narrow green beams as pump beams and one spectrally-broad red beam as the Stokes beam. The frequency difference between the green and red beams typically corresponds to the vibrational Raman shift of  $\text{N}_2$ . The CARS signal is then a faint, spectrally-broad blue beam that contains the  $\text{N}_2$  spectrum. This spectrum can be detected and then fit with a theoretical model on a computer to determine the temperature.

The dual-pump CARS technique used here differs from the typical single-pump CARS technique because it uses two different colors for the pump beam: one green and the other yellow. The same broadband red beam is used as in conventional broadband  $\text{N}_2$  CARS. The frequency of the yellow pump beam is chosen so that the frequency difference between the yellow and red beams equals a vibrational Raman resonance of  $\text{O}_2$ , with the green and red beams probing the  $\text{N}_2$  vibrational Raman transitions. The resulting blue CARS spectrum contains both  $\text{N}_2$  and  $\text{O}_2$  spectra. The relative intensities of these two spectra provide a measure of the relative mole fractions of  $\text{N}_2$  and  $\text{O}_2$ .

Coincidentally, several pure-rotational Raman transitions of  $\text{H}_2$  are present in these spectral regions as well, as described in detail in Ref. 25. These  $\text{H}_2$  transitions are also measured in the present experiment, allowing, in principle, the relative mole fractions of  $\text{N}_2$ ,  $\text{O}_2$  and  $\text{H}_2$  to be quantified simultaneously. Mole fractions of  $\text{H}_2$  are not presented herein due to unresolved difficulties in analysis of the data.

A planar BoxCARS phase-matching geometry was used, with the green and red beams overlapping. The probing volume formed at the intersection of the three beams had a minimum diameter of  $130 \mu\text{m}$  full width half maximum (FWHM), measured by traversing a knife-edge across the foci of all three beams. The probe volume is 1.8 mm long (FWHM). The measurement volume could be moved in the y and z direction within the duct by a system of prisms on translating vertical and horizontal stages. Data were acquired as a series of instantaneous (laser pulse duration  $\sim 10$  ns) measurements along either a vertical or horizontal line in the flow. The order and direction of these scans was randomized to defend against systematic errors caused by factors like heating of the duct during a facility run. Locations of the data points have been plotted in Fig. 5. This figure is a cutaway view of the duct (top and left sidewalls are removed), looking upstream from above.

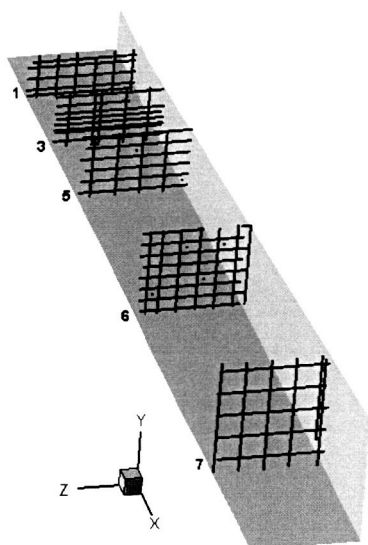


**Figure 5 CARS data point locations.**

The CARS system was characterized by making measurements in an atmospheric-pressure furnace and a  $H_2$ -air laminar flat-flame burner.<sup>24</sup> Temperatures in the flame could be measured with a single-shot standard deviation of  $\sim 70$  K over the entire temperature range, and mean measurements agreed with an adiabatic calculation to within  $\pm 60$  K. Mole fractions for  $N_2$  agreed with the computation to within the average single-acquisition standard deviation of 0.027, with an average absolute difference between the measurement and the calculation of 0.010. Measured  $O_2$  mole fractions also agreed with the prediction within the average single-shot standard deviation of 0.026 with an average absolute difference between the measurement and the calculation of 0.009.

After the CARS spectra were processed to determine the temperature and species mole fractions at various locations in the duct, response surfaces were fit to these data to provide quantitative maps of the mean flowfield parameters. These fits, by virtue of their limited number of fit coefficients (much less than the number of data points), smooth (or average) the data. Using these fitted surfaces to determine mean values of the flowfield parameters one can then compute statistics of the fluctuations in the measured parameters<sup>20,23</sup>. The difference between each measured sample and the mean, denoted by a primed quantity such as  $T'$  for temperature fluctuations and  $\chi_i'$  for fluctuations of mole fraction species  $i$ , and the chosen fluctuation product, such as  $T'T'$ , is found. The fluctuation product data are then fit to a response surface, as described above, to provide an estimation of the distribution of mean values of the product. In this way, mean square fluctuations or cross

products, such as  $\overline{T'T'}$  or  $\overline{T'\chi_{N_2}'}$  are calculated.

In the experiments we shall describe, 2000-3000 data points were acquired for each plane. The statistical uncertainties associated with generating the mean surface fits are typically twice as big as the systematic errors discovered during the flame and furnace calibration studies. It would probably have been worthwhile to acquire up to twice the number of data point per plane to reduce these uncertainties in line with the uncertainties in the flame measurements. Uncertainties are as high as  $\pm 20\%$  of peak values in mean square fluctuations or cross products. This high uncertainty is primarily due to insufficient data points, rather than instrument precision. For example, to reduce the uncertainty by one half would require 4 times as much data. However, the data is included as proof that such measurements can be made with the current system.

### **CFD CALCULATION**

The CFD calculations presented in this paper have been extensively described in Ref. 27. Only a brief summary will be presented here.

The nozzle was simulated separately and the results used as inflow conditions for the combustor calculation.

The inlet boundary was modeled as subsonic inflow, with a total pressure and temperature of 767250 Pa and 1828 K, respectively. These values were assigned based on 1-D analysis of the flow in the combustor and nozzle, based on known flow rates of reactants and the nozzle throat area, as described in Ref. 20. The inflow turbulence intensity  $\tau$  (ratio of velocity turbulent-fluctuations over mean-velocity) and turbulent-to-laminar viscosity-ratio  $\mu_t/\mu_l$  were set at the inlet to give respectively 2.5% and 300 at the nozzle exit. In addition to this baseline, high/low turbulence cases were considered with 3.5%/1.5% and 850/100 for these parameters. Wilcox's 1998  $\tilde{k} - \tilde{\omega}$  model and wall-matching functions were used for modeling turbulent viscous stresses and heat-transfer; the turbulent Prandtl number ( $Pr_t$ ) was assumed to be 0.90.

A reference solution for the combustor was obtained to provide a first approximation to the problem, and from which parametric studies could be done. The chemistry model used was Drummond's 9-specie/18-reaction ( $9 \times 18$ ) mechanism<sup>37</sup>; The Wilcox  $\tilde{k} - \tilde{\omega}$  turbulence model and wall functions were again used. They were supplemented with the Wilcox compressibility correction, but the Pope correction for the round-jet/plane-jet anomaly was not used. The turbulence Prandtl ( $Pr_t$ ) and Schmidt ( $Sc_t$ ) numbers were set to 1.0.

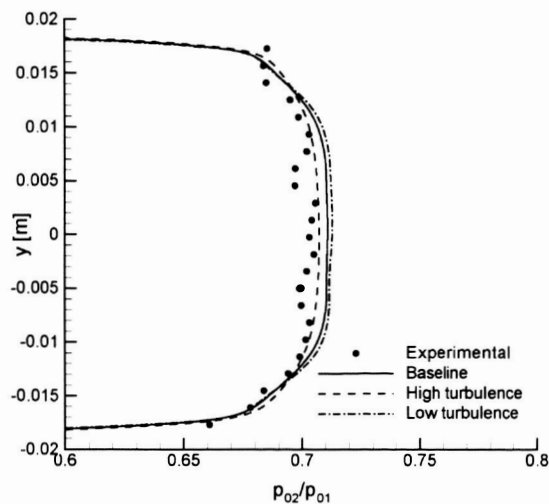


**Figure 6 DCSCTF  $M=2$  nozzle exit vertical-centerplane Pitot pressure profile from Ref. 34, and calculations.**

### RESULTS - NOZZLE EXIT

The experimental Pitot-profiles for the nozzle-exit vertical centerplane are compared with the calculations in Fig. 6. All 3 calculations fall within the 1% error bounds for the Pitot data. However, the high turbulence case gives the best results and there is little difference between the low turbulence case and the baseline.

CARS surveys were not performed at the exit of the nozzle, but plane 1 is located ahead of injection of fuel and therefore may substitute for an inflow plane, or at least be used to verify the nozzle flow conditions. Figure 7 show the results of all the CARS surveys at plane 1 plotted versus spanwise position. Also shown are the CFD values at the horizontal symmetry plane. The predicted conditions, based on 1-D calculations of the nozzle flow and the gas inflow rates to the heater, are  $T=1187\pm60$  K,  $\chi_{O_2}=0.187$  and  $\chi_{N_2}=0.513$ .<sup>20</sup> Taking the average across the duct between  $z=\pm40$  mm, the measured properties are  $T=1250$  K,  $\chi_{O_2}=0.204$  and  $\chi_{N_2}=0.494$  with standard deviations of 151 K, 0.024 and 0.042 respectively. These measurements are in reasonable agreement: the calculated values fall within one standard deviation of the measurements, but the measurement mean does not quite fall within the 95% uncertainty limits of the calculation. The temperature standard deviation is more than twice the 70 K measured in the laminar flame (Ref. 24), which indicates that the variations in freestream temperature are large enough to be resolved by the CARS system. If we assume that the temperature fluctuation is independent of instrument precision error, then these add in quadrature

and we can obtain an upper limit of 130 K as the standard deviation of the facility plane 1 temperature.

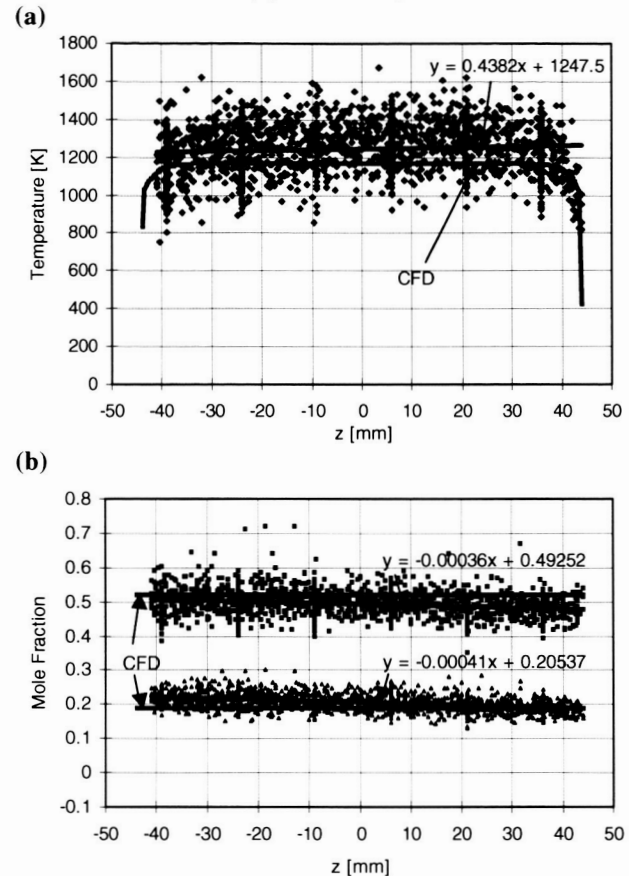


**Figure 7 All CARS surveys at plane 1 (at various  $y$ ), straight line fit, and CFD result at horizontal symmetry plane: (a)  $T$  (K), (b)  $\chi_{N_2}$  (red squares) and  $\chi_{O_2}$  (green triangles).**

The measured standard deviation in the freestream mole fractions are similar to the measurement standard deviation of the technique in laminar flame, so the real fluctuations cannot be resolved in this experiment. Note also the slightly nonuniform distribution of both  $O_2$  and  $N_2$  mole fraction, with decreasing concentration with increasing  $z$ . This is not an artifact of the heating of the facility during each run because care was taken to traverse the duct in both positive and negative  $z$ -directions to prevent such systematic errors.

The likely presence of such high temperature fluctuations ( $\sim 10\%$ ) is of concern because there are likely then to also be large velocity fluctuations. Fluid particles of different temperatures (and consequently density) tend to be accelerated at different rates in the nozzle. If one considers a simple-minded thought experiment in which the hotter and cooler particles in the nozzle flow are

segregated into 2 ideal steady streams (assumed of equal ratio of specific heats and molecular weight), and experience the same imposed streamwise pressure gradient, the percentage difference in velocity between the streams at the nozzle exit is one half that of the percentage difference in temperature. The true situation in the nozzle is a little different, since the flow entering the nozzle is turbulent, with hotter and cooler eddies intermingled, but the result is suggestive. The effect is manifest in the turbulent kinetic energy equation by the pressure work term,  $\frac{\overline{\rho' u'} \partial \bar{p}}{\bar{\rho} \partial x}$ , which is zero in incompressible flows but would be large in this nozzle flow. This term is typically not modeled. Note that  $u'/\bar{u} \sim 3\text{-}5\%$  at the nozzle exit would have significant effects on the mixing of fuel in the combustor.

### COMBUSTOR RESULTS

Experimental and calculated results for  $T$ ,  $\chi_{N_2}$  and  $\chi_{O_2}$  are presented in Fig. 8. Note that injection is from the top wall, between planes 1 and 3, and flow is from top left to bottom right.

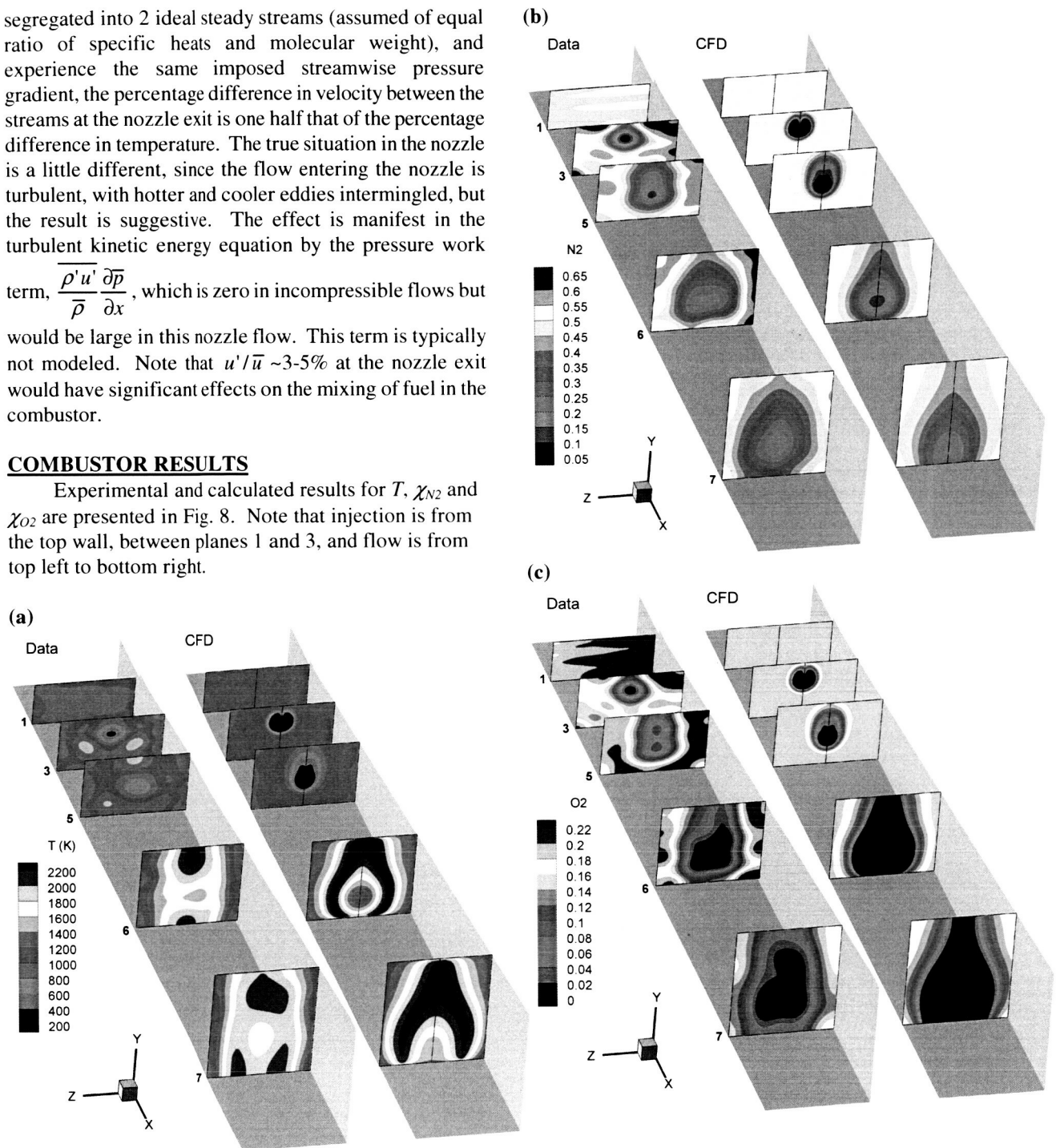


**Figure 8 Comparison of CARS and CFD results: (a)  $T$ , (b)  $\chi_{N_2}$  and (c)  $\chi_{O_2}$ .**

The  $H_2$  jet first becomes visible in plane 3 as a region of low  $T$ ,  $\chi_{N_2}$  and  $\chi_{O_2}$ . The first indications of combustion occur at the top of the duct in plane 5, where the temperature increases to a peak value of



approximately 1600-1700 K, compared to 800-900 K for the same location in the mixing-only experiment of Ref. 25 (see Fig. 9). The fact that combustion is already occurring in plane 5 is of interest, because there was some concern that the flow was igniting at the joint between the copper and stainless steel ducts; but plane 5 is ahead of this junction. As noted in Ref. 20, the temperature fluctuations in the plume at plane 5 are much higher than anywhere else in the flow. It is speculated that the combustion at this location is relatively intermittent, and far from equilibrium in the mean. At planes 6 and 7 the combustion has rapidly progressed, and is much closer to equilibrium in the mean. The minimum of the  $O_2$  mole fraction is much lower in planes 6 and 7 than at plane 5. The measured temperature distributions at all planes look very similar to those obtained previously (Ref. 20), despite nearly two years having elapsed between the sets of measurements, and the introduction of many new components in the CARS measurement system.

Comparisons between the measurements and CFD lead to the following observations. (i) The CFD shows little sign of chemical reaction until plane 6, with a very abrupt progression of reaction between the planes 5 and 6, whereas the experiment shows signs of intermittent reaction at plane 5, and a smoother, slower, progression of reaction. (ii) The experiment suggests less reaction at planes 6 and 7 than the CFD (lower temperatures, and more  $O_2$  in the plume). (iii) The CFD predicts greater fuel penetration than is observed in the experiment. (iv) The fuel plume is more diffuse in the experiment at the upstream planes. This may in part be real, perhaps due to more rapid mixing of the flow, or intermittency (flapping of the jet). However, we also suspect that the experiment does not properly resolve the flow here due to insufficient data relative to the steep gradients in the flow, and the inability of the response function to fit them.

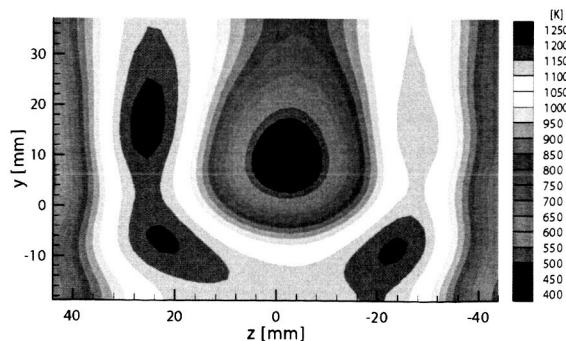
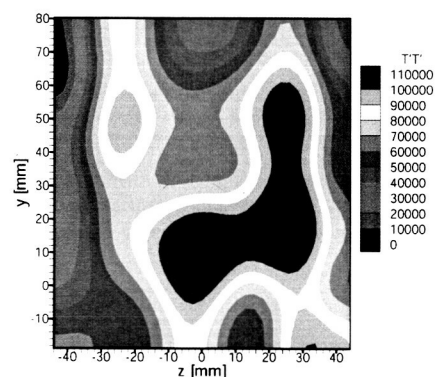


**Figure 9** CARS temperatures at plane 5 for mixing, no-combustion experiment, Ref. 25 (note the different color scale vs. Fig 6(a)).

The effects of several parameters of the CFD model

were studied in Ref. 27. Lowering  $Sc_T$ , i.e., increasing species diffusion, had little impact on fuel-plume penetration, but the ignition occurred too far upstream and pressure-rise predictions were unacceptable. On the other hand, a lower  $Pr_T$  (higher thermal-energy diffusion) had little effect on pressure-rise and ignition-delay while having a somewhat lower penetration of the fuel-plume. The effects of the different combinations of inflow turbulence were considered. The high-turbulence inflow condition, which appeared to give better agreement with the nozzle data, was shown to give a somewhat better approximation to jet-penetration, but the ignition occurred too far upstream. The low-turbulence inflow had ignition too far downstream, and pressure rise was underpredicted. One common thread through all these calculations is the apparent inability of current turbulence-modeling to accurately predict ignition delay, combustion pressure-rise and fuel-plume penetration simultaneously. So far, only two of the three parameters at best could be adequately captured.

(a)



(b)

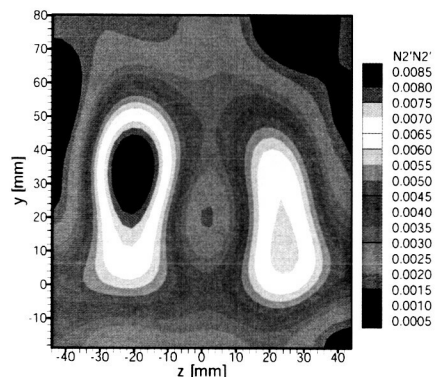


**Figure 10** CARS fluctuating measurements at plane 7:

(a)  $\overline{T'T'}$  (b)  $\overline{\chi_{N2}'\chi_{N2}'}$

Figure 10 shows some typical turbulent fluctuation correlations at plane 7. As previously described, this data is only illustrative since insufficient data points have



resulted in relatively high uncertainty. Fluctuations are generally high in regions where the gradient of the mean quantity is high, although it is not clear why temperature fluctuations are high near the bottom of the fuel plume, while the concentration fluctuations are not.

### **DISCUSSION AND CONCLUSIONS**

In the axisymmetric jet experiment it has been shown how high quality mean flow data can be used to set empirical constants in turbulence models. This case also shows the limitations of mean flow data for this purpose. There is insufficient information to resolve some of the modeling issues – for example, the compressibility correction and the turbulent kinetic energy diffusion coefficient have sufficiently similar effects that they cannot be independently chosen. One approach is to perform multiple experiments at different conditions. However, in the end, such an approach cannot be expected to work if the underlying models are incorrect. The other approach is to measure turbulent quantities in order to obtain the additional information required. Indeed, even only a little such information can provide useful insights, as was found with the RELIEF measurements of streamwise velocity fluctuations.

In the supersonic combustor experiment it was found that the data obtained were totally insufficient for setting the multiple turbulence flow parameters and models, and indeed this experiment was not intended for that purpose. One would expect that most of these parameters would be set by reference to more simple flows, and that an experiment such as this would be reserved for verifying the proper behavior of models, or for identifying general areas of deficiency. However, the true state of affairs is that there is considerable uncertainty in the appropriate values for constants such as turbulent Prandtl and Schmidt number. Indeed, these quantities may have to be treated as variables to be modeled. Another result evident from this experiment is the uncertainty inherent in the chemical kinetics model and/or problems associated with the non-use of a model to account for turbulence-chemistry interactions. It was found that choosing parameters of turbulence modeling to produce the correct fuel plume penetration caused the ignition location to move too far upstream. Furthermore, the ignition region (the region of rapid temperature rise) was much shorter in the calculation than appeared to be the case in the experiment.

A shortcoming of the experiment was noted in that inflow turbulence levels were not fully quantified, and that inflow turbulent kinetic energy levels may have been high enough to significantly affect the mixing in the combustor.

Finally, it is concluded that supersonic combustion experiments of intermediate complexity between the coaxial jet and the supersonic combustor are needed to

resolve many of the modeling issues and allow constants for the models to be set. Ideally, such an experiment would be part of a sequence in which additional affects and complexity are added one after another. For example, an axisymmetric jet without combustion, one with combustion but flameholding at the nozzle exit (to eliminate ignition modeling issues), and finally one with flame standoff due to ignition delay. Detailed measurements should include inflow and jet turbulence quantities.

### **REFERENCES**

- <sup>1</sup> Drummond, J.P., Cockrell, C.E., Jr., Pellett, G.L., Diskin, G.S., Auslender, A.H., Exton, R.J., Guy, R.W., Hoppe, J.C., Puster, R.L., R. Rogers, R.C., Trexler, C.A., Voland, R.T., *Hypersonic Airbreathing Propulsion – An Aerodynamics, Aerothermodynamics, and Acoustics Competency White Paper*, NASA/TM-2002-211951, Nov. 2002.
- <sup>2</sup> Papamoschou, D., Roshko, A., "The compressible turbulent shear layer: an experimental study," *J. Fluid Mech.*, Vol. 197, pp. 453-477, 1988.
- <sup>3</sup> Dimotakis, P., "Turbulent Free Shear Layer Mixing and Combustion," in Murthy, S.N.B., Curran, E.T. (eds.), *High-Speed Flight Propulsion Systems*, *AIAA Progress in Astronautics and Aeronautics Series*, Vol. 137, 1991.
- <sup>4</sup> Rossmann, T., Mungal, M.G., Hanson, R.K., "Evolution and growth of large-scale structures in high compressibility mixing layers," *J. of Turbulence*, Vol. 3, No.9, pp. 1-18, 2002.
- <sup>5</sup> Urban, W.D., Watanabe, S., Mungal, M.G., "Velocity field of the planar shear layer - Compressibility effects," *AIAA Paper 98-0697*, *AIAA, Aerospace Sciences Meeting & Exhibit*, 36th, Reno, NV, Jan. 12-15, 1998.
- <sup>6</sup> Island, T.C., Urban, W.D., Mungal, M.G., "Quantitative scalar measurements in compressible mixing layers," *AIAA Paper 96-0685*, *AIAA, Aerospace Sciences Meeting and Exhibit*, 34th, Reno, NV, Jan. 15-18, 1996.
- <sup>7</sup> Panda, J., Seasholtz, R.G., "Density fluctuation measurement in supersonic fully expanded jets using Rayleigh scattering," *AIAA Paper 99-1870*, *AIAA Space Technology Conference & Exposition*, Albuquerque, NM, Sept. 28-30, 1999.
- <sup>8</sup> Seasholtz, R.G., Panda, J., Elam, K.A., "Rayleigh scattering diagnostic for measurement of velocity and density fluctuation spectra," *AIAA Paper 2002-0827*, *AIAA Aerospace Sciences Meeting & Exhibit*, 40th, Reno, NV, Jan. 14-17, 2002.
- <sup>9</sup> Panda, J., Seasholtz, R., Elam, K., "Measurement of Correlation Between Flow Density, Velocity and Density\*velocity<sup>2</sup> with Far Field Noise in High Speed Jets," *AIAA Paper 2002-2485*, *8th AIAA/CEAS Aeroacoustics Conference & Exhibit*, Breckenridge, CO, 17-19 June, 2002.
- <sup>10</sup> McDaniel, J. C., Jr., "Combustor data bases for hypersonic airbreathing propulsion systems," *AIAA Paper 98-1646*, *AIAA International Space Planes and Hypersonic Systems and Technologies Conference*, 8th, Norfolk, VA, Apr. 27-30, 1998.
- <sup>11</sup> McDaniel, J.C., Fletcher, D.G., Hartfield, Jr., R.J., Hollo, S.D., "Staged Transverse Injection into Mach 2 Flow behind a Rearward-Facing Step: A 3-D Compressible Test Case for

Hypersonic Combustor Code Validation," AIAA Paper 91-5071, Dec. 1991.

<sup>12</sup> Goyne, C.P., McDaniel, J.C., Krauss, R.H., Day, S.W., "Velocity measurement in a dual-mode supersonic combustor using particle image velocimetry," AIAA Paper 2001-1761, AIAA/NAL-NASDA-ISAS International Space Planes and Hypersonic Systems and Technologies Conference, 10th, Kyoto, Japan, Apr. 24-27, 2001.

<sup>13</sup> Santoro, R.J., Pal, S., Woodward, R.D., Schaaf, L., "Rocket Testing at University Facilities," AIAA Paper 2001-0748, 39<sup>th</sup> Aerospace Sciences Meeting, Reno, NV, Jan. 8-11, 2001.

<sup>14</sup> Lehman, M., Pal, S., Broda, J.C., Santoro, R.J., "Raman Spectroscopy Based Study of RBCC Ejector Mode Performance," AIAA Paper 99-0090, 37<sup>th</sup> Aerospace Sciences Meeting, Reno, NV, Jan. 11-14, 1999.

<sup>15</sup> Bresson, A., Bouchardy, P., Magre, P., Grisch, F., "OH/acetone PLIF and CARS thermometry in a supersonic reactive layer," AIAA Paper 2001-1759, AIAA/NAL-NASDA-ISAS International Space Planes and Hypersonic Systems and Technologies Conference, 10th, Kyoto, Japan, Apr. 24-27, 2001.

<sup>16</sup> Cutler, A. D., Carty, A. A., Doerner, S. E., Diskin, G. S., Drummond, J. P., "Supersonic Coaxial Jet Flow Experiment for CFD Code Validation," AIAA 99-3588, 30<sup>th</sup> AIAA Fluid Dynamics Conference, Norfolk, VA, June 28-July 1, 1999.

<sup>17</sup> Cutler, A. D., Diskin, G. S., Danehy, P. M., Drummond, J. P., "Fundamental Mixing and Combustion Experiments for Propelled Hypersonic Flight," AIAA Paper 2002-3879, 38<sup>th</sup> AIAA/ASME/SAE/ASEE Joint Propulsion Conference and Exhibit, Indianapolis, Indiana, July 7-10, 2002.

<sup>18</sup> Cutler, A. D., White, J. A., "An Experimental and CFD Study of a Supersonic Coaxial Jet," AIAA Paper 2001-0143, 39<sup>th</sup> Aerospace Sciences Meeting, Reno, NV, Jan. 8-11, 2001.

<sup>19</sup> Drummond, J. P., Diskin, G. S., Cutler, A. D., Danehy, P. M., "Fuel-Air Mixing and Combustion in Scramjets," AIAA Paper 2002-3878, 38<sup>th</sup> AIAA/ASME/SAE/ASEE Joint Propulsion Conference and Exhibit, Indianapolis, Indiana, July 7-10, 2002.

<sup>20</sup> Cutler, A. D., Danehy, P. M., Springer, R. R., O'Byrne, S., Capriotti, D. P., DeLoach, R., "Coherent Anti-Stokes Raman Spectroscopic Thermometry in a Supersonic Combustor," *AIAA J.*, Vol. 41, No. 12, pp. 2451-2459, 2003.

<sup>21</sup> *Direct-Connect Supersonic Combustion Facility, Facility Brochure*, Wind Tunnel Enterprise, NASA Langley Research Center, [www.wte.larc.nasa.gov](http://www.wte.larc.nasa.gov).

<sup>22</sup> Danehy, P. M., DeLoach, R., Cutler, A. D., "Application of Modern Design of Experiments to CARS Thermometry in a Model Scramjet Engine," AIAA Paper 2002-2914, 22<sup>nd</sup> AIAA Aerodynamic Measurement Technology and Ground Testing Conference, St. Louis, MO, June 24-26, 2002.

<sup>23</sup> Danehy, P.M., Dorrington, A.A., Cutler, A.D. and DeLoach, R., "Response surface methods for spatially-resolved optical measurement techniques," AIAA 2003-0648, 41<sup>st</sup> Aerospace Sciences Meeting and Exhibit, Reno, Nevada, January 2003.

<sup>24</sup> O'Byrne, S., Danehy, P.M., Cutler, A.D., "N<sub>2</sub>/O<sub>2</sub>/H<sub>2</sub> Dual-Pump CARS: Validation Experiments," 20<sup>th</sup> International Congress on Instrumentation in Aerospace Simulation Facilities, Göttingen, Germany, Aug. 25-29, 2003.

<sup>25</sup> Danehy, P.M., O'Byrne, S., Cutler, A.D., Rodriguez, C.G.,

"Coherent Anti-Stokes Raman Scattering (CARS) as a Probe for Supersonic Hydrogen-Fuel/Air Mixing," JANNAF APS/CS/PSHS/MSS Joint Meeting, Colorado Springs, CO, Dec. 1-5, 2003.

<sup>26</sup> O'Byrne, S., Danehy, P. M., Cutler, A. D., "Dual-Pump CARS Thermometry and Species Concentration Measurements in a Supersonic Combustor," AIAA Paper 2004-0710, 42<sup>nd</sup> Aerosciences Meeting and Exhibit, Reno NV, Jan 5-8, 2004.

<sup>27</sup> Rodriguez, C.G., Cutler, A.D., "CFD Analysis of the SCHOLAR Scramjet Model," AIAA Paper 2003-7039, AIAA 12<sup>th</sup> International Space Planes & Hypersonic Systems & Technologies Conference, 15-18 Dec., 2003.

<sup>28</sup> White, J. A., Morrison, J. H., "A Pseudo-Temporal Multi-Grid Relaxation Scheme for Solving the Parabolized Navier-Stokes Equations," AIAA Paper 99-3360, June 1999.

<sup>29</sup> Wilcox, D. C., *Turbulence Modeling for CFD*, 2<sup>nd</sup> Edition, DCW Industries, Inc., July 1998.

<sup>30</sup> Bagheri, N., Strataridakis, C.J., White, B.R., "Turbulent Prandtl Number and Space-Time Temperature Correlation Measurements in an Incompressible Turbulent Boundary Layer," AIAA Paper 90-0020, 28<sup>th</sup> Aerospace Sciences Meeting, Reno, NV, Jan. 8-11, 1990.

<sup>31</sup> Calhoon, W.H., Jr., Kannepalli, C., Papp, J.L., Dash, S.M., "Analysis of Scalar Fluctuations at High Convective Mach Numbers," AIAA Paper 2002-1087, 40<sup>th</sup> Aerospace Sciences Meeting, Reno, NV, Jan. 14-17, 2002.

<sup>32</sup> Diskin, G. S., "Experimental and Theoretical Investigation of the Physical Processes Important to the RELIEF Flow Tagging Diagnostic," Ph.D. Dissertation, Princeton University, 1997.

<sup>33</sup> *Design-Expert® Software, Version 5.0, User's Guide*, Stat-Ease Inc., 1998.

<sup>34</sup> Springer, R. R., Cutler, A. D., Diskin, G. S., Smith, M. W., "Conventional/Laser Diagnostics to Assess Flow Quality in a Combustion-Heated Facility," AIAA Paper 99-2170, 35<sup>th</sup> AIAA/ASME/SAE/ASEE Joint Propulsion Conference and Exhibit, Los Angeles, CA, June 20-24, 1999.

<sup>35</sup> Lucht, R.P., "Three-laser coherent anti-Stokes Raman scattering measurements of two species," *Optics Letters*, Vol. 12, No. 2, February 1987, pp. 78-80.

<sup>36</sup> Hancock, R.D., Schauer, F.R., Lucht, R.P. and Farrow, R.L., "Dual-pump coherent anti-Stokes Raman scattering measurements of nitrogen and oxygen in a laminar jet diffusion flame," *Applied Optics*, Vol. 36, No. 15, 1997.

<sup>37</sup> Drummond, J.P., "A Two-Dimensional Numerical Simulation of a Supersonic, Chemically Reacting Mixing Layer", NASA TM 4055, 1988.